CORROSION SCIENCE AND TECHNOLOGY, Vol.10, No.5(2011), pp.162~166

Development of Al-added High Strength Galvannealed Daul Phase Steel Sheets

Dong-Eun Kim†, Young-Chul Han, Heung Seok Ko[1], Jong-Gi Kim[1], and Man-Been Moon

Hyundai HYSCO, 313, Donggok-ri, Songsan-myeon, Dangjin-gun, Chungnam-do, Korea
[1]Chonbuk National University, 567 Baekje-daero, Deokjin-gu, Jeonju-si, Jeollabuk-do, Korea
(Received October 20, 2009; Revised October 31, 2011; Accepted October 31, 2011)

Effects of chemical compositions and manufacturing conditions on mechanical properties and microstructures were investigated in order to obtain galvannealed high strength dual phase steel sheets with superior mechanical properties and coating properties. An intercritical annealing between Ac1 and Ac3 was conducted to produce the DP (dual phase) steel sheets, followed by quenching to room temperature. The purposes of Al addition are to reduce the iron oxidation with chemical composition (Si, Mn etc.) and to improve the wettability by liquid zinc.
The present study will focus on the characterization for making dual phase steel sheets and enhancing the galvanizability of Al added DP steel sheets about continuous annealing line in CGL.

Keywords *: DP steel sheets, AHSS, Galvannealed, heat treatment, low yield ratio*

1. Introduction

In order to reduce vehicular greenhouse emissions, the light-weight of cars is a major issue for the automotive industry. However, this light-weight can not be attained at the cost of mechanical properties or crashworthiness.[1)] In response to these needs, Advanced High Strength Steels (AHSS) were designed and developed by steel makers for automotive applications.[2)] Dual-Phase (DP) steel sheets are one of the most common AHSS steel sheets. The higher initial work hardening rate with excellent uniform and total elongation combines to give DP steel sheets a much higher ultimate tensile strength(UTS) and a lower ratio of yield strength(YS) to UTS than conventional steel sheets or high-strength low-alloy(HSLA) steel sheets at a similar level of yield strength These characteristics have made DP steel sheets attractive for automotive applications.[3)] As the circumstances exposed to automotive are also getting severe due to chloride for snow removing, air pollution and acid rain. The assurance period for corrosion protection of car body is getting longer, coated steels particularly hot dip galvanized steels having benefits for heavy coating with low operational cost are increasingly being applied to automotive use.[4)] Galvannealed steel sheets are being used increasingly for applications requiring excellent corrosion resistance, paintability and weldability, such as automotive body panels. Galvannealed coating, however, is consisted of brittle intermetallics, so coating failure has been one of concerns with galvannealed coating. The coating failure is thought to be classified into two modes : the internal failure caused in the coating and the interface failure caused at the coating/steel interface. Therefore, Galvannealed dual phase steel sheets of mechanical properties are achieved through intercritical annealing followed by quenching with N2-H2 and N2 gas atmosphere to avoid selective oxide. The reaction between Fe and Zn can be accelerated by galvannealing at high temperature. However, high temperature galvannealing leads to deterioration of the coating adhesion.[5)] In order to accelerate the galvannealing reaction, a lot of means had been examined up to date: surface activation by oxidation-reduction,[6)] 2-step annealing separated by pickling to remove the selective surface oxides,[7)] surface modification of the cold-rolled steel surface by Fe electroplating.[8)] The galvanizing reaction on steel sheets proceeds by immersion of solid steel into Zn. The reaction temperature, around 460 ℃, evidently high for Zn, which is kept in its melted state, remains quite low for steel sheets whose melting point are 1536 ℃. That means that atoms transportation in steel is far slower than atoms transportation into liquid Zn. The consequence is that local equilibrium along interfaces between solid steel and liquid zinc is set by the thermodynamic

† Corresponding author: gggff4252@hysco.com

state of zinc, the liquid phase.

In this report, in order to develop the galvannealed AHSS dual phase steel sheets with addition of chemical composition for good coating properties, surface modification by the heat treatment was studied.[9)-10)]

2. Experimental

2.1 Materials and heat treatment

Experimental Ingots made about 20 kg in laboratory by vacuum induction furnace. They were homogenized at 1250 ℃ for 2 hours in Argon atmosphere and then hot rolled to 2.6 mm hot band. Finishing Temperatures were kept above 900 ℃ and coiling temperatures were kept at 600 ℃ for 30 minutes, then air cooled to ambient temperature. After pickling in 10% hydrochloric solution at 80 ℃, steel sheets are then cold rolled to 1.0 mm thick. The cold rolled steel sheets were annealed with heat treatment conditions as shown Fig. 1 by heat treatment equipment to simulate annealing at intercritical temperature and it was selected through Ac1, Ac3 and Ms temperatures which were estimated from available equations.[11)-12)]

The composition of the steel substrates investigated is listed in Table 1. Mechanical Properties are tested by Tensile test. Microstructures and the surface of coating layer are observed in a field emission gun scanning electron microscope (FEG-SEM) and Focused Ion Beam(FIB). Coating Properties were investigated with coating profiles by glow discharge spectrometry (GDS)

$$Ac1\ (℃) = 723 - 10.7Mn + 29.1Si$$

$$Ac3\ (℃) = 910 - 203(C^{1/2}) + 44.7Si$$

$$Ms\ (℃) = 539 - 423C - 30.4Mn - 7.5Si + 30Al$$

3. Results and discussion

3.1 Microstructure and mechanical properties

Microstructures of hot rolled steel sheets were composed of ferrite and pearlite with band morphology. The band morphology was disappeared by heat treatment in the intercritical region. Microstructures of DP steel sheets

Table 1. Chemical Composition (wt.%)

Content	C	Si	Mn	Al	Mo	Cr	Ac1 (℃)	Ac3 (℃)	Ms (℃)
CB1	0.05~0.09	0.1~0.3	1.0~2.0	-	-	0.2	711	913	433
AM2				0.5	0.1	-	707	906	449

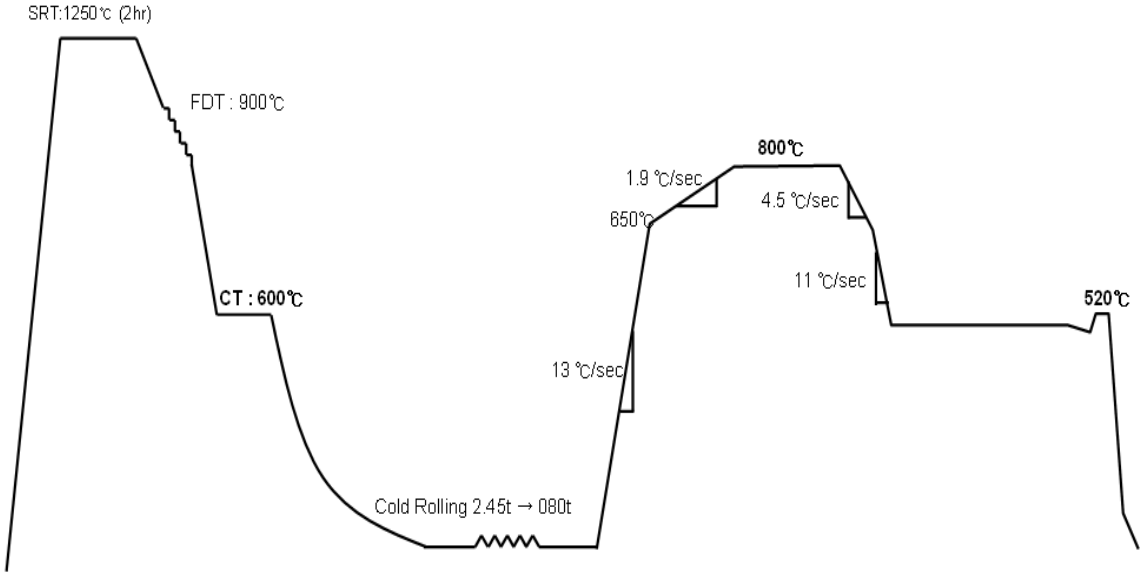

Fig. 1. Schematic illustration of the process parameters.

are shown Fig. 2. DP steel sheets were composed of ferrite and martensite phases. Fine structure of ferrite and smaller ferrite volume was achieved as the intercritical annealing temperature was increased. This was because more austenite was formed at higher intercritical annealing temperature and the austenite was transformed to martensite during quenching. Fig. 2 shows the general dual phase structure which volume fractions of martensite for CB1 and AM2 are 11% and 15%, respectively after heat treatment within intercritical temperature. Fig. 2 (c) shows expanded microstructures by Fig. 2 (b).

Martensite phase shows island type in intergranualar or grain boundaries. Fig. 3 shows martensite morphology. Fig. 3 (a) shows martensite phase among ferrite grain boundaries as shown ⓐ and also shows dislocation around. However, ⓑ shows other phases partially like bainite similar to pearlite except ferrite and martensite which size is about 0.5 ㎛. Fig. 3 (b) shows AM2 steel sheets which are similar to martensite around ferrite grain boundaries like Fig. 3 (a) and it exhibites martensite phases around grain boundariesby ⓒ in Fig. 3 (b). Also, Fig. 3(b) ⓓ shows movable dislocations around exhibited by advanced high strength steel sheets (AHSS) dual phase.

Mechanical Properties and martensite volume fraction of DP steel are shown in Table 2. The value of CB1 and AM2 is shown as a comparison. Their mechanical properties are similar to those of 590 MPa grade steel sheets and Elongation of CB1 is 28% which is higher than that of AM2, and YR is almost equal, however, YR of CB1 is higher than AM2 just a little.

3.2 Galvannealed coating properties

In GA baths, Al level ranges between 0.125 and 0.135 wt.%, at 460 ℃. The solid phase in thermodynamic equilibrium with the liquid phase is now Al saturated δ phase. When the coated steel sheet is subjected to galvannealing,

Table 2. Mechanical Properties of CB1 and AM2

	YS (MPa)	TS (MPa)	Elongation (%)	YR	Martensite Vol. fraction (%)
CB1	402	624	28	0.64	11
AM2	392	655	25	0.60	15

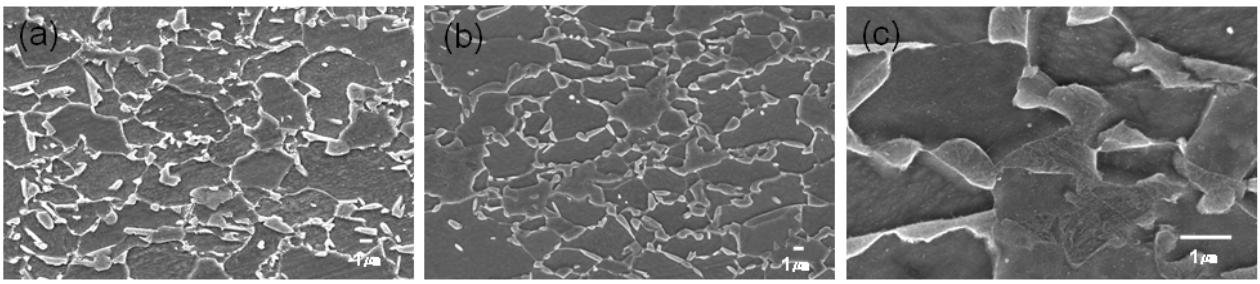

Fig. 2. SEM Microstructures of CB1 (a) X3,000, AM2 (b) X3,000 and (C) X15,000.

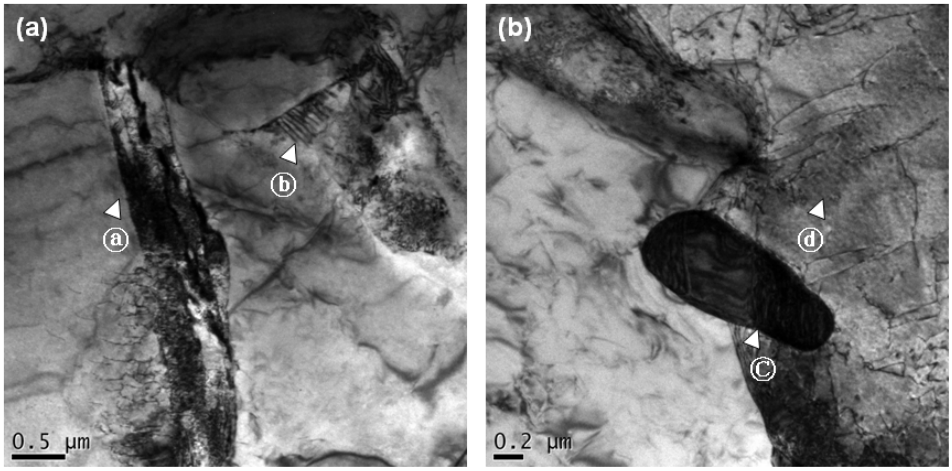

Fig. 3. TEM Microstructures of CB1 (a), AM2 (b).

the coating would solidify through constitutional supercooling, namely isothermal solidification, resulting from the enrichment of the liquid coating with iron due to the Fe-Zn interdiffusion. The remaining liquid coating would then be solidified by decreasing temperature (physical cooling) for short galvannealing or by constitutional supercooling for longer galvannealing. The surface morphology and microstructure is an example of the solidification by constitutional supercooling followed by physical cooling. The σ crystals are formed from liquid through constitutional supercooling, and the remaining liquid solidified to form the η phase by physical cooling. (Fig. 4 (a)-(b))

Voids are always found to be located near the surface of the galvannealed coatings, once the σ phase reached the surface of the coating. The voids are thought to form due to solidification shrinkage. The solidification must have occurred first near the coating/substrate interface and propagated to the coating surface due to the concentration gradient. This resulted in the location of the voids near the coating surface, where the last portion of liqiid in the coating surface, where the last portion of liquid in the coating to be solidified, as the solidification is driven by constitutional supercooling instead of physical cooling. The solid state interdiffusion governs the change in microstructure of galvannealed coatings only when the solidification completes by constitutional supercooling before the end of the galvannealed process. The effect of the liquid state diffusion must be the dominating process in determining the iron distribution in the coating. As iron continues to diffuse toward the surface region, the above mode of solidification continues to completion. Consequently, well-defined crystals of the σ phase form on the coating surface. The facts that the early formation of σ crystals visible on the surface and the similarity among the surface morphologies of the solidification must have completed in this mode in the early stages of galvannealing. The voids formed at the last stage of solidification are annealed out gradually by the vacancy diffusion mechanism for longer galvannealing.

Fig. 6 (a) and (b) show the GDS peaks with the chemical compositon of the substrate. Here it should be noted that the change with depth was different with Al content of the chemical composition in the substrate. Fig. 6 (a) shows the typical depth profiles on the surface and at the interface.

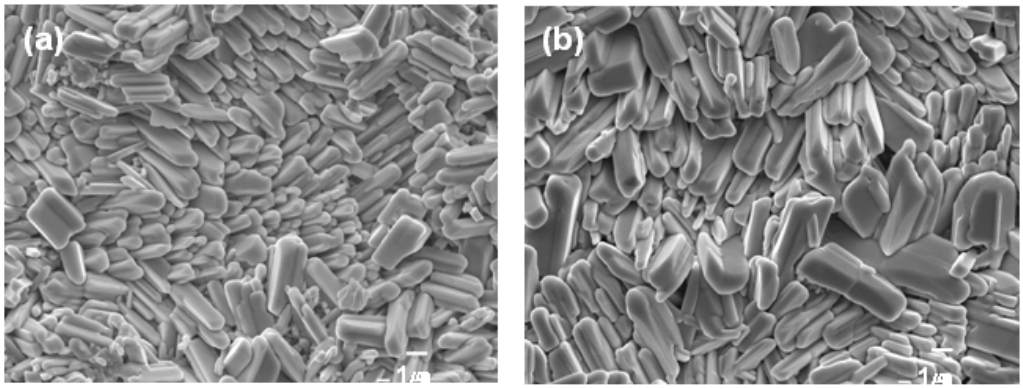

Fig. 4. FEG-SEM images of galvannealed surface (a) CB1 and (b) AM2.

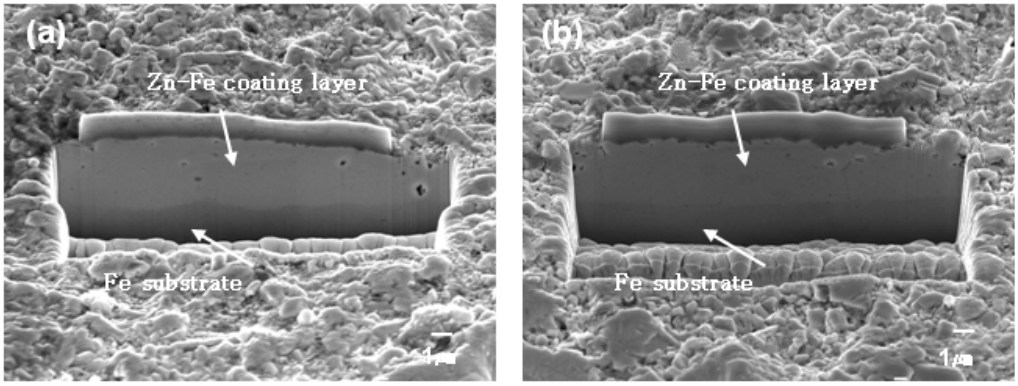

Fig. 5. FIB Images of Galvannealed Surface (a) CB1 (b) AM2.

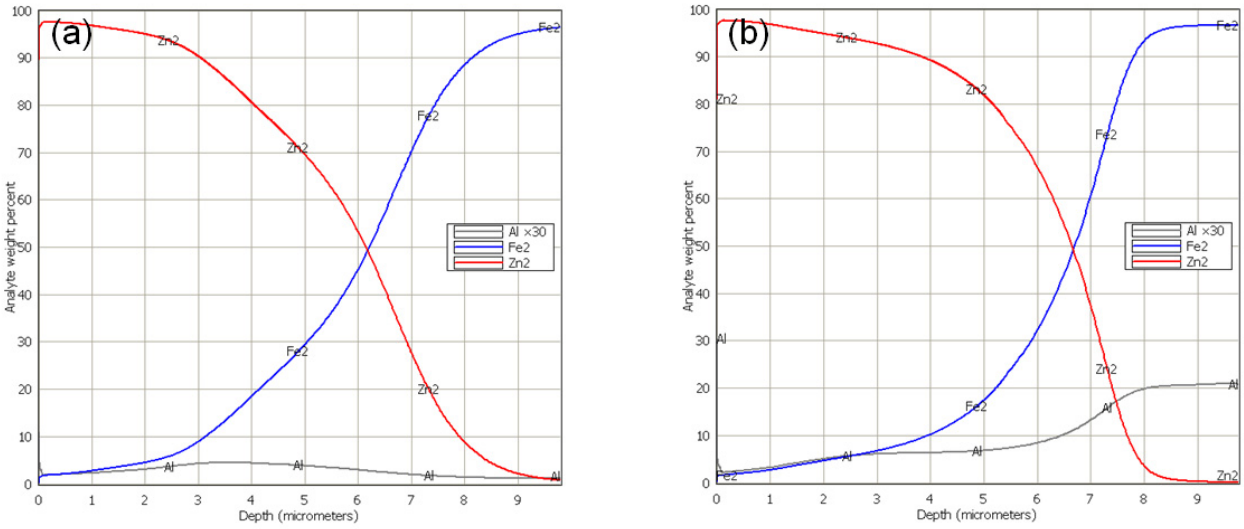

Fig. 6. GDS of Depth Profile (a) CB1 (b) AM2.

However, Fig. 6 (b) shows the increase of Al content at the interface.

4. Summary

The mechanical and coating properties between CB1 and AM2 have been investigated and results are summarized as follow:

1) The tensile strength of dual phase galvaannealed steel sheets is higher than 590 MPa, and elongation is above 25 %.

2) The coating layer is about 10 ㎛ and the similar coating properties as those of conventional mild steel sheets

3) The coating layer of CB1 shows more cavities with chemical composition of DP galvannealed steel compared to AM2.

4) CB1 steel sheets have general depth profile, but AM2 steel sheets have increased Al depth profile with Al addition in chemical compositions

References

1. B. Mintz, *Int. Rev.*, **46**, 169 (2001).
2. C. D. Horvath and J. R. Fekete, Proceedings of *International Conference on Advanced High Strength Sheet Steels for Automotive Applications*, p. 3, AIST, Warrendale, USA (2004).
3. Technical Transfer Dispatch #6-Body Structure Materials, *UlSAB-AVC Consortium* (2001).
4. M. B. Moon and W. B. KIM, *GALVATECH '07*, p. 363 (2007).
5. M. Sakurai, L. W. Zhang, Y. Tajiri, and T. Kondo, *Tetsu-to Hagane*, **77**, 1 (1998).
6. A. Komatsu, A. Ando, and T. Kittaka, *Nisshin Seiko Giho*, **77**, 1 (1998).
7. N. Fujibayashi, Y. Tobiyama, and K. Kyono, *CAMP-ISIJ*, **10**, 609 (1997).
8. T. Ooi, A. Takase, M. Ohmura, and S. Shimada, *CAMP-ISIJ*, **7**, 603 (1994).
9. Y. Suzuki and Y. Kyono, *Hyomen-gijutu*, **55**, 48 (2004).
10. Y. Suzuki, Y. Sugimoto, and S. Fujita, *Hyomen-gijutu*, **58**, 183 (2007).
11. J. G. Speer, A. M. Streicher, D. K. Matlock, F. Rizzo, and G. Krauss, *ISS/TMS*, 505 (2003).
12. K. W. Andrews, *J. Iron and Steel Inst.,* **203**, 721 (1965).